anism of action of a variety of structurally more complex antibiotics.

References

Anbar, M., & Neta, P. (1967) *Int. J. Appl. Radiat. Isot. 18*, 493.

Auld, D. S., Kawaguchi, H., Livingston, D. M., & Vallee, B. L. (1974) *Proc. Natl. Acad. Sci. U.S.A. 71*, 2091.

Chang, L. M. S., & Bollum, F. J. (1970) *Proc. Natl. Acad. Sci. U.S.A. 65*, 1041.

Downey, K. M., Que, B. G., & So, A. G. (1980) *Biochem. Biophys. Res. Commun. 93*, 264.

Fong, K., McCay, P. B., Poyer, J. F., Misra, H. P., & Keele, B. B. (1976) *Chem.-Biol. Interact. 15*, 77.

Haber, F., & Weiss, J. (1934) *Proc.—R. Soc. Edinburgh, Sect. A 147*, 332.

Halliwell, B. (1976) *FEBS Lett. 72*, 8.

Kobashi, K., & Horecker, B. L. (1967) *Arch. Biochem. Biophys. 121*, 178.

Lown, J. W., & Sim, S.-K. (1976) *Can. J. Biochem. 54*, 446.

Lown, J. W., & Sim, S.-K. (1977) *Biochem. Biophys. Res. Commun. 77*, 1150.

Lown, J. W., Sim, S.-K., Majumidar, K. C., & Chang, R.-Y. (1977) *Biochem. Biophys. Res. Commun. 76*, 705.

Lown, J. W., Sim, S.-K., & Chen, H. H. (1978) *Can. J. Biochem. 56*, 1042.

McClune, G. J., & Fee, J. A. (1976) *FEBS Lett. 67*, 294.

Mildvan, A. S. (1974) *Annu. Rev. Biochem. 43*, 357.

Misra, H. P. (1974) *J. Biol. Chem. 249*, 2151.

Modrich, P., & Lehman, I. R. (1970) *J. Biol. Chem. 245*, 4756.

Oberley, L. W., & Buettner, G. R. (1979) *FEBS Lett. 97*, 47.

Poiesz, B. J., Seal, G., & Loeb, L. A. (1974) *Proc. Natl. Acad. Sci. U.S.A. 71*, 4892.

Que, B. G., Downey, K. M., & So, A. G. (1979) *Biochemistry 18*, 2064.

Roots, R., & Okada, S. (1975) *Rad. Res. 64*, 306.

Sausville, F. A., Stein, R. W., Peisach, J., & Horwitz, S. B. (1978a) *Biochemistry 17*, 2746.

Sausville, F. A., Peisach, J., & Horwitz, S. B. (1978b) *Biochemistry 17*, 2740.

Scrutton, M. C., Wu, C. W., & Goldthwaite, D. A. (1971) *Proc. Natl. Acad. Sci. U.S.A. 68*, 2497.

Sigman, D. S., Graham, D. R., D'Aurora, V., & Stern, A. M. (1979) *J. Biol. Chem. 254*, 12269.

Sim, S.-K., & Lown, J. W. (1978) *Biochem. Biophys. Res. Commun. 81*, 99.

Slater, J. P., Tamin, I., Loeb, L. A., & Mildvan, A. S. (1972) *J. Biol. Chem. 247*, 6748.

Springgate, C. F., Mildvan, A. S., Abramson, R., Engle, J. L., & Loeb, L. A. (1973) *J. Biol. Chem. 248*, 5987.

Van Hemmen, J. J., & Meuling, W. J. S. (1977) *Arch. Biochem. Biophys. 182*, 743.

Walling, C. (1975) *Acc. Chem. Res. 8*, 125.

Interaction of Aluminum Species with Deoxyribonucleic Acid†

S. J. Karlik,* G. L. Eichhorn,* P. N. Lewis,* and D. R. Crapper*

ABSTRACT: Interactions of aluminum with deoxyribonucleic acid (DNA) have been studied by thermal denaturation, circular dichroism, and fluorescent dye binding; a pH- and concentration-dependent alteration in the interaction of aluminum with DNA was observed. Three distinguishable complexes are produced when DNA is denaturated at pH 5.0–7.5 and in aluminum to DNA mole ratios of 0–0.7. Complex I appears at neutral pH and stabilizes a portion of DNA. Complex II is observed at acidic pH, destabilizes a fraction of the DNA double-helical molecule, and produces intrastrand cross-links. Complex III occurs at all pHs, is maximal at intermediate pH values, and is characterized by a noncooperative melting profile and cross-linking at low pH (<6.0). The DNA in complexes II and III can be renatured by treatment with either ethylenediaminetetraacetic acid (EDTA) or a high concentration of sodium chloride. The properties of complexes I and II are consistent with what could be expected for DNA complexes of $Al(OH)^{2+}$ and Al^{3+}, respectively. Complex III has intermediate properties that are consistent with a structure in which both ions bind the DNA simultaneously. The characteristics of complex III depend on the ratio of Al^{3+}/$Al(OH)^{2+}$ in solution. Aluminum–DNA complexes differ from other metal–DNA complexes in that melting profiles under many conditions are biphasic. Apparently more than one form of DNA can exist at any time in the presence of aluminum. The different DNA–aluminum complexes, which arise from the multiple species of aluminum in aqueous solution, lead to a variety of reactions with DNA.

Recent interest in the biological role of aluminum has been stimulated by the discovery that increased amounts of this metal occur in several human brain diseases. These conditions include Alzheimer's disease (Crapper et al., 1973, 1976; Trapp et al., 1978), dialysis encephalopathy (Alfrey et al., 1976; Arieff et al., 1979), and ALS-Parkinson dementia in Guam and Kii peninsula (Yase, 1977; Yoshimasu et al., 1976). Aluminum levels in normal human brain were also found to be significantly increased during aging (McDermott et al., 1979).

Alzheimer's disease is the most prevalent form of senile dementia and accounts for from 50 to 70% of such disorders (Butler, 1978; Terry, 1978). There is now substantial evidence that the disease is accompanied by localized depositions of aluminum in brain cells. Such deposition has been observed by histochemical techniques (DeBoni et al., 1974; Crapper &

† From the Departments of Physiology (S.J.K. and D.R.C.) and Biochemistry (P.N.L.), University of Toronto, Toronto, Canada M5S 1A8, and the National Institutes of Health, National Institute on Aging, Gerontology Research Center (G.L.E.), Baltimore City Hospitals, Baltimore, Maryland 21224. *Received March 3, 1980.* S.J.K. was awarded an Ontario Mental Health Foundation Studentship.

This article not subject to U.S. Copyright. Published 1980 by the American Chemical Society

DeBoni, 1977; Crapper et al., 1980) and recently confirmed by X-ray spectrometry (Perl & Brody, 1980). These studies also reveal that the Al accumulation is in the chromatin of the cell nuclei. It is therefore of potential importance to an understanding of some aspects of Alzheimer's disease to elucidate the interaction of aluminum with DNA.

Previous studies on the interaction of DNA with a variety of metal ions have shown that some metal ions bind preferentially to the bases, others to phosphate, and still others to both sites. The reactions of aluminum are complicated by the existence of aluminum as different species in aqueous solution. Thus, the effects of aluminum depend upon the nature of the species present under a given set of conditions.

Materials and Methods

Chemicals. All solutions were prepared from analytical grade salts and doubly distilled water. Aluminum is found in many reagents and care was taken to prevent contamination; precipitation on glass was not uncommon. Therefore nalgene plasticware was employed. Aluminum concentrations were determined by atomic absorption (Crapper et al., 1976). Unhydroxylated aluminum ions were added to experimental solutions from a 0.1 M aluminum chloride solution (pH 2.0) (Baes & Mesmer, 1976). Calf thymus (CT) DNA (Sigma Type I) was dissolved in water by shaking for 24–48 h at 4 °C in a gentle rotary mixer. The protein content was <0.2% as assayed by the Lowry method (Lowry et al., 1951). DNA concentrations were routinely measured spectrophotometrically by employing an ϵ_{260} of 6000 M^{-1} cm^{-1} and are reported throughout this paper in terms of *nucleotide residue*. The concentrations in DNA stock solutions were also measured with the Burton assay (Burton, 1956). Ethidium bromide (3,8-diamino-6-phenyl-5-ethylphenanthidinium bromide) (Sigma Chemical Co.) had an extinction coefficient, ϵ_{480}, of 5450 M^{-1} cm^{-1} (Le Pecq, 1971).

Thermal Denaturation. Melting experiments were performed on a Gilford 2400 recording spectrophotometer and a Pye-Unicam SP500 spectrophotometer adapted for computerized data collection. The Gilford was equipped with an automatic cuvette programmer, thermosensor, and multichannel recorder. A Haake thermostat F was used in conjunction with a synchronous motor to provide a constant heating and cooling rate of 0.3 and 1.0 °C/min, respectively, through the integral thermal plates. Derivative curves of the thermal denaturation experiments were obtained from the computer-adapted Unicam single-beam spectrophotometer (Lewis, 1977). The data were digitized by a 14 bit A to D converter, interfaced through a CAMAC system to a PDP 11 computer. A Yellow Springs Instrument thermistor probe (No. 421) and telethermometer were used to determine the intracuvette temperature. The temperature detector was calibrated against a precision thermometer and was employed to calibrate the Gilford platinum thermosensor. Thermal derivative curves were obtained from an IBM 360/75 11-point cubit fit of a minimum of 150 data points. Spurious electrical transients were deleted. For minimization of scattering artifacts, denaturation experiments were always observed at 320 nm at the beginning and end of the experiments and occasionally entire denaturation experiments were recorded at 320 nm when the aluminum concentration was high.

Derivative experiments were repeated several times (up to six). Curves observed at high pH and all aluminum concentrations were easily reproducible. At pH <6.5, however, and especially at 0.5 mole ratio of aluminum and greater, the reproducibility was dependent on the accurate adjustment of the initial pH. Although the overall profiles were generally unchanged, a difference of 0.10 pH units could result in alterations of height and position for individual subtransitions.

Fluorescence Emission. Aliquots of thermal denaturation solutions were heated to 99 °C for 5 min in sealed containers and cooled slowly (1.5 h) to room temperature. Fluorescence emission measurements at 595 nm were performed on an Aminco SPF-500 fluorometer by employing an excitation wavelength of 365 nm (Karsten & Wollenberger, 1977). Measurements were corrected for lamp fluctuations and scattering artifacts, and blanks were the identical solutions without ethidium bromide. Ethidium bromide (EB) alters DNA melting (LePecq & Paoletti, 1967) and in the studies involving denatured DNA was therefore added after the solutions had been denatured. The optimum mole ratio for EB fluorescence was 0.2 (mol of EB/DNA) for all solutions; to favor intercalation binding this mole ratio was not exceeded. The emission wavelength maximum was unperturbed by the addition of aluminum. The fluorescence of the DNA–aluminum solutions was expressed as a percentage of that produced by uncomplexed DNA at the same pH.

Ultraviolet and Circular Dichroism Measurements. The Gilford and Unicam spectrophotometers were used for routine ultraviolet measurements, and spectral scans were recorded on a Bausch and Lomb 505 dual-beam spectrophotometer. The aluminum–ethylenediaminetetraacetic acid (EDTA) molar extinction was extremely low and did not alter the UV data. The circular dichroism spectra were recorded on a Jasco J-41 spectropolarimeter at 20 °C by using stoppered 1-cm cylindrical cells.

pH Measurements. The pH was measured on a Radiometer pHM standard digital pH meter. Sodium hydroxide (10 mM) and nitric acid (10 mM) were used to adjust the initial pH of the experimental solutions, and final pHs were recorded after cooling to room temperature.

Data Analysis. To facilitate analysis of the data, we divided the experimental temperature range into four regions: (A) 35–50, (B) 51–64, (C) 65–80, (D) >80 °C.

Individual peaks in the derivative melting profiles were specified by (a) initial pH, (b) aluminum/DNA mole ratio, and (c) T_m, range or temperature value. For example, (5.0, 0.4, 41.6) identifies the low-temperature melting peak in the A range observed in the biphasic DNA derivative profile at pH 5.0, aluminum/DNA mole ratio of 0.4, at a temperature of 41.6 °C (Figure 1). To quantitate the thermal melting curves for presentation in Figure 3, we expressed the hyperchromicity between inflection points on the integral curves as a fraction of the total hyperchromicity of that denaturation experiment. The curve illustrated for (5.0, 0.7, 64.0) was omitted from Figure 3 for reasons outlined under Discussion.

Results

Thermal Denaturation. Calf thymus DNA was denatured in 5×10^{-3} M sodium nitrate in the presence of aluminum varying from mole ratio 0.0 to 0.7 and initial pH from 5.0 to 7.5 (Figure 1). Melting and cooling curves for aluminum–DNA solutions at various pHs have been also presented in Figure 2. At Al/DNA mole ratios of 0.3 and greater, aluminum induced three changes in the melting profile of DNA: (1) the single monophasic transition was divided into several smaller peaks occurring at various temperatures (Figure 1); (2) the melting temperature range was increased (Figure 2B–D); (3) the fraction of DNA denatured at 95 °C was reduced (Figure 2B–D). In addition, when DNA solutions in the presence of high aluminum were cooled to room temperature, the absorbance failed to decrease (Figure 2C,D). Although transitions could be observed in the conventional

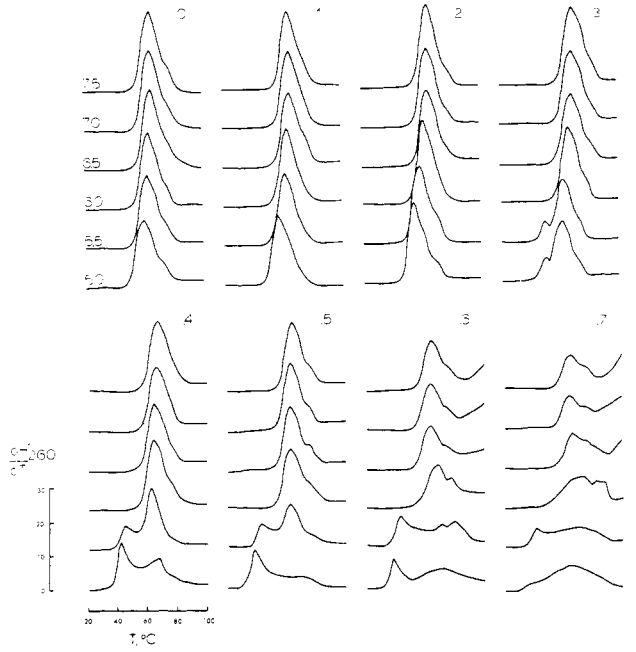

FIGURE 1: Derivative thermal denaturation of 6×10^{-5} M DNA (in 5×10^{-3} M $NaNO_3$) in the presence of aluminum concentrations from 0 to 0.7 Al/DNA and from pH 5.0 to 7.5. $dH'/dT = 1000(dH/dT)$, where H = hyperchromicity.

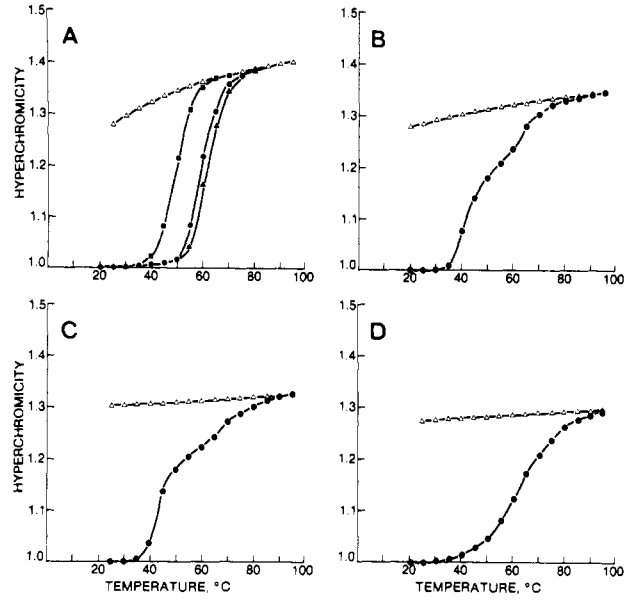

FIGURE 2: Melting (filled symbols) and cooling curves (Δ) for 6×10^{-5} M DNA (in 5×10^{-3} M $NaNO_3$): (A) (6.3, 0, B) (▲), (6.0, 0.1, B) (●), (5.8, 0.3, B) (■); (B) (5.4, 0.4, A and C); (C) (5.2, 0.5, A and C); (D) (5.0, 0.7, B). For explanation, see Data Analysis under Materials and Methods.

representations, the components were clearly delineated by plotting the derivative as shown in Figure 1.

DNA denatured in a single B-range transition for pHs in the range of 5.0–7.5 at aluminum/DNA mole ratios <0.3. The high-temperature shoulder is a property of CT DNA (Pivec et al., 1972; Guttman et al., 1977). The derivative profiles were not significantly altered, although the T_m decreased at lower pH values. The single transition remained relatively unchanged above pH 6.0 and Al/DNA ratios between 0.3 and 0.5. Beyond this range of pH and aluminum concentrations, marked alterations in the DNA melting profile were observed.

At >0.2 mole ratio of aluminum and at pH <6.0, a low-temperature melting peak was observed in the A range. This

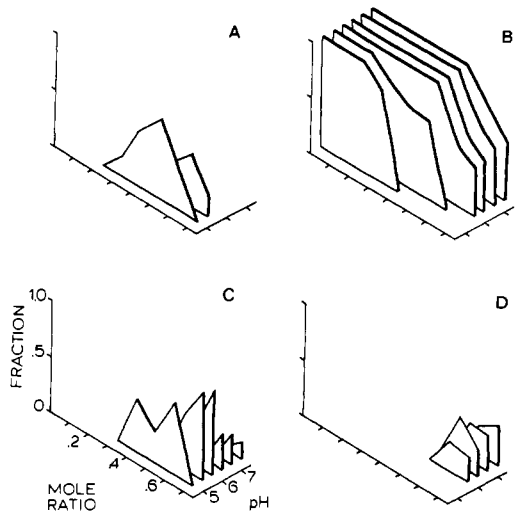

FIGURE 3: Fraction of hyperchromicity from denaturation curves illustrated in Figure 1 contained in transitions occurring in temperature regions described under Materials and Methods: (A) 35–50, (B) 51–64, (C) 65–80, and (D) >80 °C.

component increased to a maximum percentage at (5.0, 0.5, 43.0) and (5.5, 0.6, 41.9) with contributions of 72 and 49% of the melting curves, respectively (Figure 3), and decreased at higher aluminum concentrations. The enlargement of the A-range peak was accompanied by a reduction in the amplitude of the B-range transition (Figure 1). With increased aluminum concentrations at low pH, the B-range peak was replaced by transitions in the higher melting C range (Figure 3).

At the lowest pH and highest aluminum concentration employed (Figures 1 and 2D), (5.0, 0.7, 64.0), the T_m was identical with that of native DNA, but the maximum dH/dT amplitude was markedly reduced and a threefold expansion of the melting temperature range was observed. The increase in melting temperature range and smaller peak amplitude were characteristics of thermal denaturation experiments at high aluminum concentrations (Figure 1).

The decreased amplitude of the B-range transition at mole ratios of 0.6 and 0.7 at high pH (6.5–7.5) was accompanied by the appearance of a steeply rising shoulder at high temperatures (Figure 1). This transition appeared incomplete within the experimental temperature range and was therefore classified in the D range (Figure 3). The biphasic melting profile at pH 6.0, mole ratio 0.6 and 0.7, contained components in the C and D ranges.

Examination of integral melting curves revealed the hyperchromicity at 95 °C decreased with increased aluminum concentrations at all pHs employed. The reduction was most apparent at low pH and high aluminum mole ratio; at (5.0, 0.7, B), the hyperchromicity at 95 °C was ~65% of that of DNA denatured in sodium nitrate alone (Figure 2).

Acidic conditions produced alterations of the DNA melting profile at lower aluminum concentrations than did more basic pHs. The A-range transition had a threshold at a mole ratio of 0.3, when the pH was <6.0 (Figure 1). Above pH 6.0, however, marked alteration of the melting profile and the production of the D-range shoulder were not observed until an aluminum mole ratio of 0.6 (Figure 1).

For all combinations of pH and aluminum illustrated in Figures 1 and 2, there was no detectable change in absorbance at 320 nm or visible precipitation. However, at 0.8 mole ratio and greater, DNA precipitation was observed during denaturation for initial pH 6.5–7.5 and at room temperature for

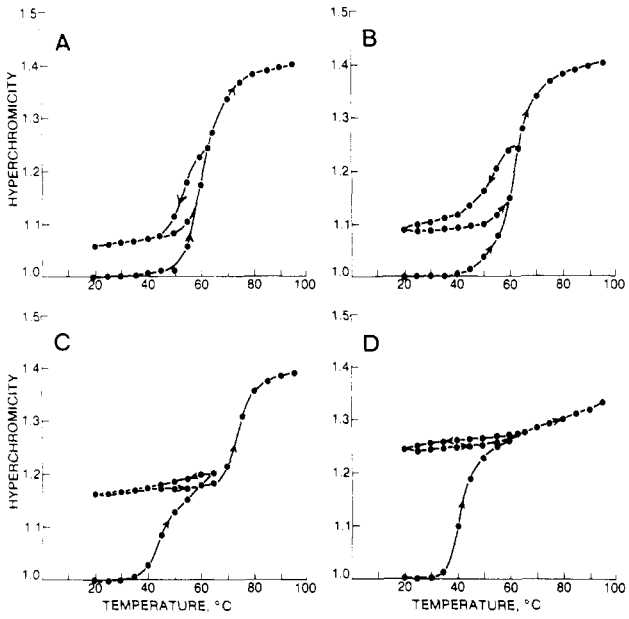

FIGURE 4: Partial-melting, cooling, and reheating curves for 6×10^{-5} M DNA in 5×10^{-3} M sodium nitrate at pH 5.5 in the presence of Al/DNA mole ratios of (A) 0, (B) 0.3, (C) 0.5, and (D) 0.6.

initial pH below 6.5. A decrease of up to 0.5 pH units (after denaturation) was observed for solutions adjusted to pHs >6.5; solutions of initial pH <6.5 rose a maximum of 0.75 pH units.

Thus the melting of DNA occurs in four distinct regions. One of these, the B region, corresponds to the melting of uncomplexed DNA, and the other three presumbly reflect different Al–DNA complexes.

Complex I, found at high aluminum concentrations and pH >6.5, is a *stabilized* complex which melts in the high-temperature portion of the denaturation temperature range. Figure 3D represents the fraction of complex I found in the thermal denaturation curves. Complex II, found at low pH (<6.0) and at aluminum mole ratios of 0.3 and greater, identifies the low-temperature melting peak observed in the A range. The quantity of this destabilized fraction of the DNA melting is illustrated in figure 3A. Complex III is characterized by a broad temperature profile with melting transitions found in the C range (Figure 3C).

The pH-dependent interconversion between these forms can be seen clearly by examination of the melting profiles for six pH values at an aluminum mole ratio of 0.6 (Figure 1). A maximum complex I transition was observed at pH 7.5 and decreased with decreased pH. A maximum complex II was observed at low pH and decreased with increased pH. Complex III was observed at all hydrogen ion concentrations. Therefore, there appears to exist a II → III → I conversion between complexes when the pH was increased from 5.0 at the same aluminum concentration.

Partial Melting. Aluminum increased the absorbance of DNA solutions partially denatured and cooled to the initial temperature (Figure 4). When DNA was denatured in the absence of Al to 64 °C (T_m) and cooled to 20 °C, the hyperchromicity after denaturation was ~1.06 (Figure 4A). At low pH (5.5), the presence of aluminum prevented the drop in absorbance observed with DNA alone.

The greater the aluminum level, the greater was the hyperchromicity; at Al/DNA mole ratios of 0.5 and 0.6, the absorbance remained at approximately the value reached when the temperature was 64 °C (Figure 4C,D). The quantity of DNA which did not renature paralleled the fraction of DNA observed in the low-temperature, A-range transition.

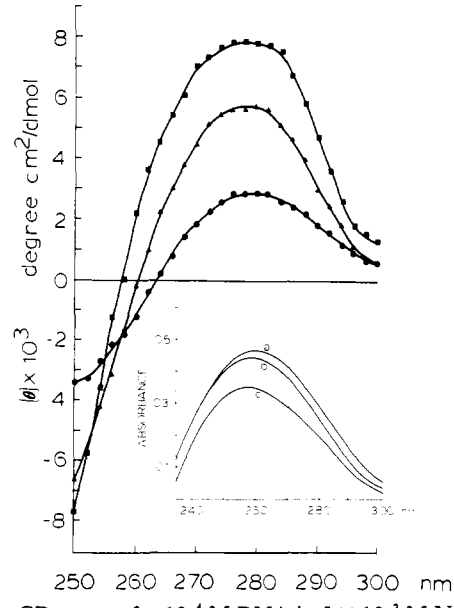

FIGURE 5: CD spectra for 10^{-4} M DNA in 5×10^{-3} M $NaNO_3$ (■) and in the presence of a 0.7 Al/DNA mole ratio, at pH 5.0 and room temperature (■); DNA solutions with and without Al heated to 95 °C and cooled to room temperature (●); EDTA (1.5 mM) added to denatured DNA alone (●) and to the aluminum–DNA solution after 2 (▲) and 4 h (■). (Insert) Absorbance spectra for 5.5×10^{-5} M DNA in 5×10^{-3} M $NaNO_3$, pH 5.0, at room temperature in the presence of 0, 0.2, 0.4, and 0.6 Al/DNA mole ratios (c). Denatured DNA in the absence of aluminum (b) and in the presence of an Al mole ratio of 0.7 (a) after cooling to room temperature; curve c also is produced from (a) 18 h after the addition of 1 mM EDTA.

In summary, an aluminum–DNA complex appeared to be generated during complex II melting which prevented the helix rewinding upon cooling that is characteristic of partially melted DNA in the absence of aluminum. Increased absorbance on cooling was also observed for uninterrupted thermal melting curves as illustrated in Figure 2C,D; thus *intra*strand hydrogen-bonding—hairpin formation—is also prevented by the presence of aluminum.

Absorption and CD Spectra. Aluminum did not change the absorption spectra of DNA solutions at room temperature up to a mole ratio of 0.7 (Figure 5c). The spectrum for denatured DNA had an increase in optical density without a change in wavelength maximum (258 nm) (Figure 5b). DNA denatured with aluminum present exhibited a somewhat greater increase in optical density after cooling than DNA alone and showed a 2-nm red shift (Figure 5a). When EDTA (final concentration 1 mM) was added to the denatured complex of (5.0, 0.7, 64.0) (figure 5a), the resulting spectrum was indistinguishable from the native DNA starting material (Figure 5c).

In the concentration range of these experiments (0–0.7), aluminum did not alter the CD spectrum (from 250 to 300 nm) for native DNA at room temperature (Figure 5). Furthermore, after denaturation (95 °C) and cooling to room temperature, the spectra for DNA with or without aluminum were not detectably different. A molar ellipticity indistinguishable from native DNA was produced by the addition of EDTA (1.5 mM) to the aluminum–DNA complex generated by denaturing DNA at a pH of 5.0 and mole ratio of 0.5. EDTA did not change the circular dichroism of DNA denatured in the absence of aluminum.

In summary, aluminum did not induce any perturbations in the CD or absorption spectra of DNA at room temperature. Although the CD for denatured DNA was identical in the presence and absence of aluminum, the UV spectra showed a red shift and an increase in absorbance. The optical prop-

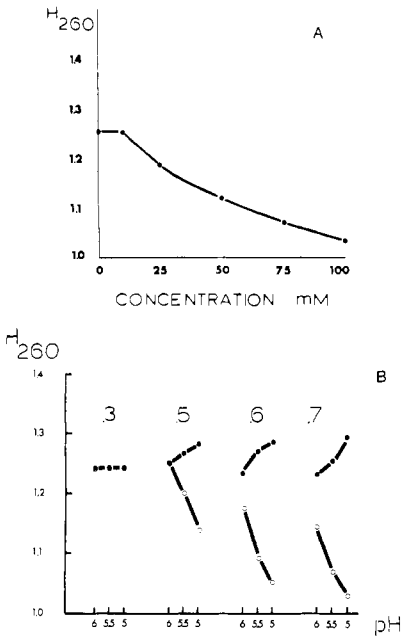

FIGURE 6: (A) Hyperchromicity of a denatured solution of 6×10^{-5} M DNA in 5×10^{-3} M $NaNO_3$ and a 0.7 Al/DNA mole ratio at pH 5.0, 18 h after the addition of solid NaCl in the concentration range of 0–100 mM. (B) Final hyperchromicity of 6×10^{-5} M DNA in 5×10^{-3} M $NaNO_3$ after denaturation and cooling in the presence of Al/DNA mole ratios from 0.3 to 0.7 and from pH 5 to 6 (●) and 18 h after the addition of 1 mM EDTA (○).

erties of denatured DNA–Al reverted to those of native DNA when the aluminum was complexed by EDTA. Thus EDTA leads to the reversal of the unwinding of DNA that takes place in the presence of aluminum; this reversal cannot be affected by cooling alone.

Final Hyperchromicity. Sodium chloride also reversed the optical density increase associated with the denaturation of DNA in the presence of aluminum. DNA was denatured under conditions which produced a prominent A-range transition (5.0, 0.6, 41.9), and the A_{260} was monitored 18 h after the addition of solid sodium chloride in the concentration range of 5–100 mM (Figure 6A). The addition of increasing quantities of NaCl to the DNA–aluminum complex resulted in a reduction in optical density. At 100 mM, the hyperchromicity was 1.04, indicating nearly complete reversal of the absorbance change associated with denaturation. As already noted, EDTA also decreased the optical density of aluminum–DNA solutions which had been denatured. The filled circles in Figure 6B represent the hyperchromicity of solutions which had been denatured and cooled to 20 °C, as illustrated in Figure 2. The Al in the complex generated at high aluminum concentration and low pH is not removed by lowering the temperature, as is evident by the retention of the increased absorbance at room temperature. The addition of EDTA, however, produced a marked decrease in the postdenaturation hyperchromicity at Al/DNA ratios exceeding 0.3 and pH <6.0 (Figure 6B, open circles). The reduction in A_{260} with EDTA increased with both the decrease in pH and the increase in aluminum concentration. The addition of EDTA failed to alter the A_{260} of solutions which denatured in a B-range transition (Figure 6B, 0.2, open circles).

Therefore, the experiments illustrated in Figure 6B may be considered as the third phase of the denaturation and cooling sequence illustrated in Figure 2. For example, one can follow the broad melting curve in Figure 2D up to 95 °C (filled circles) and down to 20 °C along the horizontal cooling curve (open triangles). The addition of EDTA at this point would

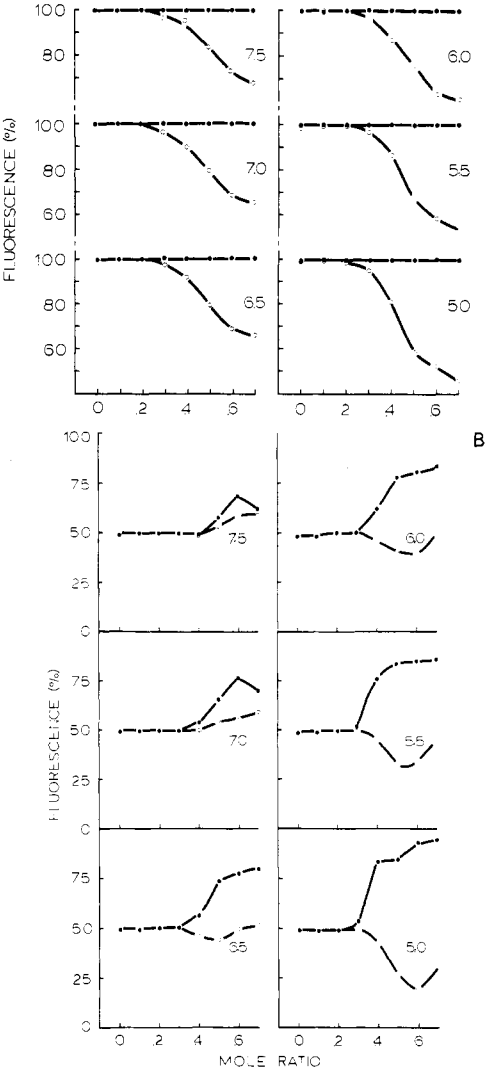

FIGURE 7: Ethidium bromide fluorescence emission for solutions combining 6×10^{-5} M DNA, 1.2×10^{-5} M ethidium bromide, and 5×10^{-3} M $NaNO_3$ in the presence of Al/DNA mole ratios from 0.1 to 0.7 expressed for (A) native and (B) denatured DNA as a percentage of the fluorescence of uncomplexed DNA, before (○) and after (●) the addition of 1 mM EDTA.

cause a decrease in absorbance to nearly the starting value, thus completing a denaturation–cooling–renaturation cycle.

In summary, reversibility can be produced by both elevated sodium chloride concentration and aluminum chelation. The extent of reversibility of Al–DNA complex formation depends on the aluminum concentration and the initial pH.

Fluorescence Emission. Ethidium bromide fluorescence with native DNA was progressively reduced by the addition of aluminum at mole ratios >0.2 and at all pHs (Figure 7A). For all Al/DNA ratios above 0.2, the fluorescence was maximal at pH 7.5 and minimal at pH 5.0. The reduction in emission was most marked at the lowest pH and highest aluminum contents (Figure 7A, open circles); at (5.0, 0.7, 64.0), the value was only 46% of that of DNA at the same pH. In all cases, the addition of EDTA to produce a 1 mM solution restored the fluorescence to 100% of that of the control (Figure 7A, filled circles) in <3 s.

DNA denatured in the absence of aluminum produced an EB fluorescence of ~50% [slightly higher than reported for ice-quenched DNA; LePecq & Paoletti (1967)]. At all pHs studied, the fluorescence was also 50% for all aluminum concentrations which resulted in B-range melting profile with the exception of (5.0, 0.7, B). The addition of EDTA did not

change the fluorescence of these solutions (Figure 7B).

At low pH and high aluminum concentrations, the fluorescence was markedly reduced. In contrast, the emission at neutral pH was increased as much as 10% above that of denatured DNA. The addition of EDTA to the latter solutions produced a small increase in fluorescence. At acidic pH the recovery of fluorescence through EDTA addition was marked, and at pH 5.0 the final value was ~95% for mole ratios 0.6 and 0.7. Eighty percent of the fluorescence was recovered in 60 s; the residual 20% took several hours.

In summary, aluminum produces an EDTA-reversible quenching of EB–DNA fluorescence with native DNA; this effect is both concentration and pH dependent. The complexes formed between aluminum and DNA during denaturation at low and high pH have a markedly reduced and slightly increased fluorescence, respectively. Only the low pH samples exhibit the marked reversal of quenching by EDTA.

Discussion

Effect of Aluminum on DNA at Room Temperature. The decrease in ethidium bromide fluorescence produced by the addition of aluminum to native DNA suggests that aluminum dissociates the dye from DNA. Le Pecq & Paoletti (1967) have shown that at <0.01 M salt concentration and at an EB/DNA mole ratio of 0.2 or less, ethidium bromide binds preferentially to intercalation sites on the DNA double helix. Thus, aluminum can dislodge EB molecules from intercalation sites. Aluminum therefore binds relatively strongly to native DNA.

However, no detectable alterations in A_{260} and ultraviolet or CD spectra were produced by the addition of aluminum to DNA at room temperature. A perturbation of base stacking by aluminum might be expected to induce changes in these optical parameters. Metal ions which have been shown to bind preferentially to the phosphate moieties on DNA (e.g., Ca^{2+}, Mg^{2+}, or Co^{2+}) do not produce modifications in the ultraviolet spectrum. The shapes of the UV spectra were altered, however, by base-binding metals such as Fe^{3+}, Cd^{2+}, or Cu^{2+} (Schreiber & Daune, 1969; Eichhorn & Shin, 1968). Alterations in CD spectra for DNA and polynucleotides have been observed for base-binding metals (Shin, 1973; Pillai & Nandi, 1977; Walter & Luck, 1977; Arya & Yang, 1975).

Taken together with the complete recovery of ethidium bromide fluorescence by chelation of the aluminum, the absence of optical alteration suggests that aluminum binds reversibly to double-helical DNA at room temperature without disturbing the hydrogen bonding.

Effect of Aluminum on Unfolding and Renaturation of DNA. In denaturation experiments above pH 6.0, the presence of a high-temperature melting shoulder in the D range and decreased hyperchromicity suggest that the major effect of aluminum at high pH is helix stabilization. The other transition is in the B range and may be attributed to uncomplexed DNA. We call this high-temperature melting species *complex I*. Many other metal ions increase the T_m of DNA, e.g., Ca^{2+}, Mg^{2+}, etc. (Eichhorn & Shin, 1968). A biphasic melting curve, however, with what appears to be free and complexed DNA melting in distinct transitions has previously been observed only when the DNA is complexed to proteins or polypeptides (Seipke et al., 1979; Subirana, 1973; Tsuboi et al., 1966; Olins et al., 1967, 1968; Li et al., 1973); it has not been observed when only metal ions are associated with the DNA. Previously examined metal ions shifted the entire melting curve to higher temperatures. Since the aluminum in complex I produces a distinct transition, it appears that portions of the DNA contain bound aluminum and others do not. Perhaps the aluminum at high pH displays preferential affinity for double-stranded rather than single-stranded DNA, and metal ion migration during the denaturation experiment (Dove & Davidson, 1962) may provide an explanation for the appearance of a distinct transition.

In denaturation experiments below pH 6.0, the B-range transition, presumably uncomplexed DNA, disappears with increasing aluminum concentrations. At a threshold of 0.3 Al/DNA mole ratio, a lower melting peak in the A range appears. The A-range peak, which we attribute to a *complex II*, decreases in amplitude with an increase in a higher melting C-range transition which is accompanied by a reduction in hyperchromicity. We call the complex melting in the C range *complex III*. Complex II displays highly cooperative melting; the complex III transition, on the other hand, is very broad. Therefore, at pH <6.0, the DNA seems to form two complexes with aluminum: complex II, which cooperatively lowers the T_m of DNA, and complex III, which noncooperatively raises the DNA melting. Again, biphasic transitions are observed, this time, at low pH. Complex II is detected as a unique, cooperative transition distinct from both complex III and uncomplexed DNA. A possible explanation for this observation is that aluminum at low pH displays a preferential affinity for unwound DNA, in contrast to the situation at high pH, where complex I appears to favor helical segments. The reduced hyperchromicity of solutions at 95 °C may be due to the presence of residual segments which do not melt or to a change in the molar extinction of the Al–DNA complexes generated during heating.

At aluminum mole ratios Al/DNA of 0.3 and greater, the complex of aluminum with DNA that is generated during denaturation is renaturable; i.e., the DNA double helix can be reformed by cooling and subsequent displacement of the Al. Maximum reconversion to double helix is observed at pH 5.0. Both complexes II and III are renaturable. Although the CD spectrum of these complexes is indistinguishable from that of denatured DNA, the increase in A_{260} and the red shift in the wavelength maximum are consistent with base binding (Eichhorn & Shin, 1968). The addition of EDTA or salt produces an increase in ethidium bromide fluorescence, reduction in A_{260}, and a return to the UV and CD spectra of native DNA. This renaturation is from 95 to 100% complete at low pH and high aluminum concentration. These observations suggest that aluminum produces cross-links between the DNA strands similar to those produced by Cu^{2+} (Eichhorn & Clark, 1965; Eichhorn & Shin, 1968). The renaturability of DNA is attributed to copper cross-links, which maintain the polynucleotide strands in register during denaturation. Cu^{2+} also lowers the T_m of DNA, but the entire thermal denaturation curve is shifted to lower temperatures, in contrast to the melting of complex II distinct from that of uncomplexed DNA produced by aluminum.

In summary, the complexes corresponding to the D-, A-, and C-range transitions[1] show the following properties. Complex I is found at high pH, stabilizes DNA and may preferentially bind to double-stranded DNA. Complex II is found at low pH, destabilizes DNA, may preferentially bind to denatured DNA, and forms cross-links between strands.

[1] The DNA melting in the B-range transition illustrated in Figure 1 (5.0, 0.7, 64) has three properties which are dissimilar to those of native DNA even though the T_m is the same. A decreased hyperchromicity at 95 °C, a broadening of the melting profile, and renaturability of the final product after denaturation clearly delineate this species from DNA melted in the absence of aluminum. Although this behavior seems compatible with complex III, this transition was omitted from Figure 3 for clarity.

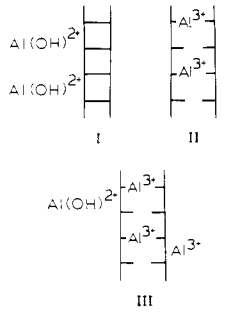

FIGURE 8: Proposed structures for aluminum complexes with DNA.

Complex III is found throughout the pH range, displays a broad melting, and exhibits pH-dependent cross-link formation, the extent of renaturability decreasing with increased pH.

pH Dependence of Aluminum–DNA Interactions. The experiments illustrated here reveal a pH-dependent dichotomy in aluminum interactions with DNA. Complex I is produced at high pH and displays the helix-stabilizing characteristics of a phosphate-binding metal such as Mg^{2+}. Complex II, in contrast, is observed at low pH and exhibits properties similar to base-binding metals, i.e., destabilization and cross-linking. The fact that a change in pH can produce an alteration in behavior suggests that this dichotomy may result from a change in the hydroxylated state of the aluminum ion; i.e., the aluminum species responsible for complex I at high pH is more hydroxylated than the aluminum species which produces complex II at low pH.

Aluminum ion (Al^{3+}), or $[Al(H_2O)_6]^{3+}$, exists in aqueous solution in a complex equilibrium with a variety of hydroxylated species. The quantity and nature of these hydroxides depends on the pH and the aluminum concentration (Baes & Mesmer, 1976). The products of aluminum hydrolysis at 10^{-5} M are five mononuclear species Al^{3+}, $Al(OH)_2^+$, $Al(OH)^{2+}$, $Al(OH)_3$, and $Al(OH)_4^-$ (these are abbreviated formulations; all the species contain coordinated water molecules) and a single isopolycation $Al_{13}O_4(OH)_{24}^{7+}$. The proportion of each of these species is, of course, pH dependent; increased pH favors the formation of more extensively hydroxylated forms. Thus, aluminum ions exist in a complex hydrolysis equilibrium even in the absence of DNA.

The neutral and negative species $Al(OH)_3$ and $Al(OH)_4^-$ would have no electrostatic attraction for DNA phosphate moieties and therefore probably do not participate in the generation of complex I. For a monopositive cation like $Al(OH)_2^+$ to produce the >90 °C T_m of complex I, it is estimated that >0.10 M $Al(OH)_2^+$ would be necessary (Dove & Davidson, 1962; Schildkraut & Lifson, 1965). The aluminum concentration in these experiments was from 10^{-6} to 10^{-5} M, far less that the amount necessary for stabilization by a monopositive cation. $Al_{13}O_4(OH)_{24}^{7+}$ may be a candidate for complex I stabilization. The electrostatic interactions of this large and highly charged cation may be expected to distort the DNA double-helical geometry by forcing a twisting or folding configuration which produces destabilization rather than stabilization.

We postulate that $Al(OH)^{2+}$ is responsible for the production of complex I and that the remaining ionic species Al^{3+} generates complex II. The concentration at which stabilization is produced by complex I approximates that necessary for similar stabilization by other divalent metals, such as Mg^{2+} (Eichhorn & Shin, 1968).

Complex III resembles in different ways both complexes I and II: its broad melting profile centered at T_m values greater than that of DNA alone suggests complex I, while the reversible denaturation, requiring cross-links, suggests complex II. We believe that these characteristics are best explained by a complex that combines features of complexes I and II, i.e., that has both Al^{3+} and $Al(OH)^{2+}$ complexed to DNA. The broad melting profile may result from the interaction of varying ratios of Al^{3+} and $Al(OH)^{2+}$. At increased aluminum concentrations, the generation of cross-links without complex II melting may also originate from the binding of Al^{3+} to both base and phosphate sites.

Figure 8 contains proposed structures for the three complexes. It must be emphasized that these structures are somewhat speculative, but some of the major features are supported by the data. The stabilization of DNA at higher pH implicates a hydroxylated aluminum species binding to phosphate (complex I). The destabilization at lower pH to form a complex from which a double helix can be regenerated (under conditions that do not lead to such regeneration in the absence of aluminum) implicates cross-linking (complex II). We postulate complex III as having a combination of the features of complexes I and II. We are presently attempting confirmation of these structures by NMR studies. It is tempting to suggest that Al cross-links could lead to deleterious biological effects, but such a conclusion requires the demonstration of such structures in chromatin in brains from Alzheimer patients.

References

Alfrey, A. C., LeGendre, G. R., & Kaehny, W. D. (1976) *N. Engl. J. Med. 294*, 184.
Arieff, A. I., Cooper, J. D., Armstrong, D., & Lazarowitz, V. C. (1979) *Ann. Intern. Med. 90*, 741.
Arya, S. K., & Yang, J. T. (1975) *Biopolymers 14*, 1847.
Baes, C. F., & Mesmer, R. E. (1976) *The Hydrolysis of Cations*, p 112, Wiley, New York, Toronto.
Burton, K. (1956) *Biochem. J. 62*, 315
Butler, R. N. (1978) *Aging (N.Y.) 7*, 5.
Crapper, D. R., & DeBoni, U. (1977) *Adv. Behav. Biol. 23*, 29.
Crapper, D. R., Krishnan, S. S., & Dalton, A. J. (1973) *Science (Washington, D.C.) 180*, 511.
Crapper, D. R., Krishnan, S. S., & Quittkat, S. (1976) *Brain 99*, 67.
Crapper, D. R., Quittkat, S., Krishnan, S., Dalton, A. J., & DeBoni, U. (1980) *Acta Neuropathol. 50*, 19.
DeBoni, U., Scott, J. W., & Crapper, D. R. (1974) *Histochemistry 40*, 31.
Dove, W. L., & Davidson, N. (1962) *J. Mol. Biol. 5*, 467.
Eichhorn, G. L., & Clark, P. (1965) *Proc. Natl. Acad. Sci. U.S.A. 53*, 586.
Eichhorn, G. L., & Shin, Y. A. (1968) *J. Am. Chem. Soc. 90*, 7323.
Guttman, T., Vitek, A., & Pivec, L. (1977) *Nucleic Acids Res. 4*, 285.
Karsten, U., & Wollenberger, A. (1977) *Anal. Biochem. 77*, 464.
Le Pecq, J. B. (1971) *Methods Biochem. Anal. 20*, 41.
Le Pecq, J. B., & Paoletti, C. (1967) *J. Mol. Biol. 27*, 87.
Lewis, P. N. (1977) *Can. J. Biochem. 55*, 736.
Li, H. J., Chang, C., & Weiskopf, M. (1973) *Biochemistry 12*, 1763.
Lowry, O. H., Rosebrough, H., Farr, A. L., & Randall, R. J. (1951) *J. Biol. Chem. 193*, 265.
McDermott, J. R., Smith, A. I., Iqbal, K., & Wisniewski, H. M. (1979) *Neurology 29*, 809.
Olins, D. E., Olins, A., & Von Hippel, P. (1967) *J. Mol. Biol. 24*, 157.

Olins, D. E., Olins, A., & Von Hippel, P. (1968) *J. Mol. Biol. 33*, 265.
Perl, D. P., & Brody, A. R. (1980) *Science (Washington, D.C.) 208*, 297.
Pillai, C. K., & Nandi, U. S. (1977) *Biochim. Biophys. Acta 474*, 11.
Pivec, L., Stokrova, J., & Somova, Z. (1972) *Biochim. Biophys. Acta 272*, 179.
Schildkraut, C., & Lifson, S. (1965) *Biopolymers 3*, 195.
Schreiber, J. P., & Daune, M. (1969) *Biopolymers 8*, 139.
Seipke, G., Arfmann, H. A., & Wagner, K. G. (1979) *Biopolymers 18*, 855.
Shin, Y. A. (1973) *Biopolymers 12*, 2459.
Subirana, J. A. (1973) *J. Mol. Biol. 74*, 363.
Terry, R. D. (1978) *Aging (N.Y.) 7*, 11.
Trapp, G. A., Miner, G. D., Zimmerman, R. L., Mastri, A. R., & Heston, L. L. (1978) *Biol. Psychiatry 13*, 709.
Tsuboi, M., Matsuo, K., & T'so, P. O. P. (1966) *J. Mol. Biol. 15*, 256.
Walter, A., & Luck, G. (1977) *Nucleic Acids Res. 4*, 539.
Yase, Y. (1977) *Exerpta Medica Int. Congr. Ser.–Excerpta Med. No. 434*, 43.
Yoshimasu, F., Uebayashi, Y., Yase, Y., Iwata, S., & Sasajima, K. (1976) *Folia Psychiatr. Neurol. Jpn. 30*, 49.

Interaction of Netropsin and Distamycin with Deoxyribonucleic Acid: Electric Dichroism Study†

Nanibhushan Dattagupta, Michael Hogan, and Donald M. Crothers*

ABSTRACT: We report dichroism and equilibrium binding studies of netropsin (Net) and distamycin A_3 (Dist) binding to deoxyribonucleic acid (DNA). We show that at low degrees of binding (r) to calf thymus DNA, Net induces a considerable increase in the apparent DNA length (14 Å/drug molecule bound), closely analogous to the results reported earlier for Dist. In addition, we show that chicken erythrocyte DNA shows length changes similar to those of calf thymus DNA upon distamycin binding. DNA length reaches a maximum at 1 bound drug/20–30 base pairs and then decreases to its initial value by $r = 0.1$. This effect is not seen for two other DNAs with nearly identical A + T base pair content and may therefore arise from the details of base sequence or base modification in eukaryotic DNA. We also show that Dist binding to calf thymus DNA at low r values is positively cooperative and shows a DNA affinity which is primarily nonionic. We demonstrate that independent of the DNA to which they are bound, the Net and Dist transition moments are inclined by 43 ± 3° from the helix axis, consistent with the idea that both drugs bind inside and parallel to the DNA small groove. From dichroism measurements, we show that the conformational change induced in calf thymus DNA by Dist does not kink or bend the helix and does not substantially alter the average inclination of the bases. Finally, we outline a statistical mechanical theory for calculation of binding isotherms when binding is coupled to a DNA structural change.

Distamycin A (Dist) and netropsin (Net) are basic oligopeptides which are potent antibacterial (Finlay et al., 1951; Thrum, 1959; Thrum et al., 1972; Sanfilippo et al., 1966), antiviral (deRatuld & Werner, 1970), and antineoplastic (DiMarco & Arcamone, 1963) agents whose pharmacological activity is based upon binding to DNA (Hahn, 1975). The binding of the two to DNA[1] shows similar properties and is by any standard quite remarkable. Both Dist and Net show a DNA binding affinity which is in some cases 100–1000 times larger than that of typical intercalating drugs, yet binding is only weakly ionic (Luck et al., 1977) and does not involve intercalation (Wartell et al., 1974); drug attachment most likely occurs outside the helix in the small groove (Wartell et al., 1974; Krey & Hahn, 1970; Kolchinskii et al., 1975). When bound, both Dist and Net induce changes in the DNA CD spectrum which have been interpreted as arising from a substantial DNA conformational alteration (Luck et al., 1974, 1977). Binding is accompanied by viscosity changes which indicate a length increase and an increase in persistence length (Luck et al., 1977; Reinert, 1972; Reinert et al., 1979), but the nature of the conformational change which occurs is unclear. In an earlier study (Hogan et al., 1979) we used the transient electric dichroism method to demonstrate a large length increase in calf thymus DNA upon Dist binding, interpreting the accompanying cooperative binding as an allosteric transformation of DNA structure. The present paper is an extension of that work.

The binding mechanisms of both Dist and Net are not understood in detail, but it is clear that they show a preference for DNA base sequence which is more complicated than any known for smaller molecules. Net and Dist are capable of preferentially inhibiting, at very low concentration, the action of endonucleases on A·T base pair rich sequences (Nosikov & Sain, 1977). CD and viscosity measurements all indicate that Net and Dist bind most tightly to A·T base pair rich regions of DNA.

Here, we describe electric dichroism and equilibrium binding studies whose goal is to define in more detail the structure of the Net and Dist complexes with DNA and to determine the kind of structural distortion they produce. Measurements were

† From the Department of Chemistry, Yale University, New Haven, Connecticut 06511. *Received May 9, 1980.* Supported by Grant CA 15583 from the National Cancer Institute.

[1] Abbreviations used: DNA, deoxyribonucleic acid; EDTA, ethylenediaminetetraacetic acid; Me_2SO, dimethyl sulfoxide; bp, base pair; CD, circular dichroism; CPK, Corey–Pauling–Koltun.

0006-2960/80/0419-5998$01.00/0 © 1980 American Chemical Society